Lasers in Surgery and Medicine 18:373–380 (1996)

Study of Corneal Ablation With Picosecond Laser Pulses at 211 nm and 263 nm

Xin-Hua Hu, PhD and T. Juhasz, PhD

Department of Physics, University of California, Irvine, California 92717

Background and Objective: **Corneal ablation has been studied by picosecond laser pulses in the far-UV region.**
Study Design/Materials and Methods: **Laser pulses of 25 ps duration at 211 nm and 263 nm wavelengths and a 1 kHz repetition rate have been used to ablate human and rabbit corneas. The dependence of the etch rate on laser fluence has been measured at both wavelengths. The collateral tissue damage has been investigated by electron microscopy.**
Results: **The ablation threshold for human cornea is determined to be about 3.0 mJ/cm^2 at 211 nm, while the thresholds for rabbit cornea are about 2.3 mJ/cm^2 at 211 nm and 8.0 mJ/cm^2 at 263 nm. The slopes of the ablation curves and the dimensions of the damage zones have also been determined.**
Conclusion: **We compare these results to the existing data on corneal ablation by nanosecond UV pulses and discuss the deficiency of the photochemical model. Experimental results are analyzed in terms of a model that features plasma ablation assisted by chromophore absorption.** © 1996 Wiley-Liss, Inc.

Key words: far-UV ablation, cornea, picosecond pulse, solid-state laser

INTRODUCTION

Corneal ablation by ultraviolet (UV) laser pulses had attracted numerous studies since the early 1980s [1–12]. It is well known that the photon energy at wavelengths near 200 nm is high enough (~6 eV) to directly break molecular bonds, which contributes to the large absorptivity in biological tissues and organic polymers. However, clear understanding of the mechanism responsible for corneal ablation by UV pulses has not been achieved. Srinivasan and coworkers have proposed that ablation in polymer materials, such as polymethyl methacrylate (PMMA), by UV laser pulses can be mainly attributed to a photochemical mechanism [13,14]. This model is based on the linear absorption by chromophores with a modification in order to take the dynamic effect of finite pulse duration into account [14]. According to the photochemical model a major part of the absorbed pulse energy channels into the formation of fragments by the decomposition of polymer molecules when the laser fluence is above the threshold level. The ablation is then accomplished by ejecting these fragments from bulk due to their high translational speed. Furthermore, the same photochemical model has been applied to corneal ablation by UV laser pulses [7–9], although water accounts for more than 70% of the wet weight of corneal tissue [15].

During the last few years measurements of laser induced fluorescence (LIF) of corneal tissues have been reported by several authors [10,11]. The results have shown that LIF of cornea illuminated by an ArF excimer laser with fluence well above the ablation threshold [11] differs considerably from that below or just above the threshold [10]. At high laser fluence the characteristics of the LIF spectrum resembles closely the blackbody radiation in the wavelength region

Accepted for publication January 19, 1995.

Address reprint requests to Dr. Xin-Hua Hu, Department of Physics, East Carolina University, Greenville, NC 27858-4353.

Xin-Hua Hu is now at Department of Physics, East Carolina University, Greenville, NC 27858-4353.

from 300 to 500 nm [11]. This quasi-blackbody characteristic of the LIF of cornea is comparable with the LIF of water when a breakdown is induced by Q-switched ruby laser pulses at 694 nm [16]. In contrast, transition between specific energy levels of excited molecules has been identified in PMMA ablated by excimer-laser pulses in a wide range of fluence [13]. The similarity between LIF from cornea and water indicates the deficiency of the photochemical model when applied to corneal ablation. Additionally, in the photochemical model the slope of the etch rate curves of cornea near threshold can be easily calculated with the absorption coefficient of the ablated material [14]. We noticed that the model calculation in the case of corneal ablation is in large disagreement with those measured by the excimer laser pulses [3,6,9] and measured by picosecond pulses in our experiment. Furthermore, a recent measurement of the spectrum of secondary radiation indicates the existence of ionized atoms at a fluence of 2 J/cm^2 in corneal ablation by an ArF excimer laser, while broadband radiation has been measured at low fluences of less than 0.5 J/cm^2 [17].

This discussion shows that the current explanation of corneal ablation by the photochemical model is not satisfactory. In this paper we report experimental results on corneal ablation by picosecond UV pulses at the 211 and 263 nm wavelengths. The dependence of etch rate, or the etch depth per pulse, on laser fluence has been investigated, and the fluence thresholds have been determined. The morphology of the collateral damage zone near the ablation site in corneal stroma has been examined using transmission electron microscopy (TEM). We discuss our data in light of previous measurements by nanosecond UV pulses and introduce an absorption-assisted plasma ablation model to interpret these experimental results.

MATERIALS AND METHODS

Figure 1 is a schematic presentation of our experiment for the UV study. A Nd:YLF oscillator/regenerative amplifier system provided laser pulses at 1,053 nm wavelength and at a 1 kHz repetition rate. The pulse duration was measured to be 50±8 ps (FWHM) with an autocorrelator. Three type I BBO crystals were used to generate the second, fourth, and fifth harmonics from the laser output [12,18]. In order to increase the conversion efficiency, the diameter of the output

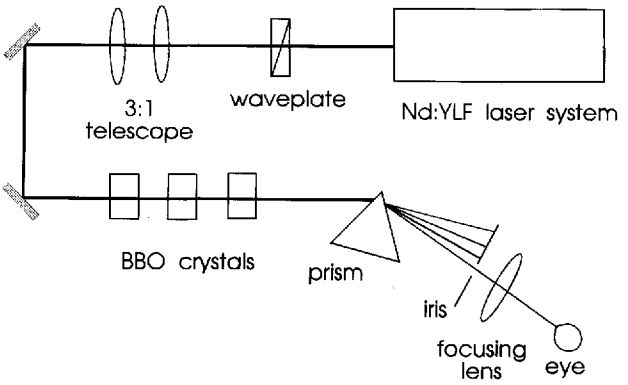

Fig. 1. Schematic diagram of the experimental setup.

beam was reduced from 3 mm to 1 mm by an inverse telescope. The average power was measured with a power meter (Gentec TPM-310) and calibrated by the spectral absorption curve of the meter at different wavelengths. The pulse energy was then obtained by dividing the average power by the 1 kHz repetition rate. The pulse energy at 1,053 nm was measured to be 1.0 mJ before entering the first BBO crystal. The fourth (263 nm) and fifth (211 nm) harmonics were generated simultaneously with pulse energies of 73 μJ and 60 μJ, respectively. The harmonics were then separated by a prism.

One of the beams was selected with an iris and focused onto a sample with a spherical lens. Lenses of different focal length from 90 to 600 μm were used to vary the spot size at the focus. The intensity distribution at the focus was measured by the knife-edge method and has been found to be close to that produced by a Gaussian beam. The diameter of the focal spot was measured at the intensity that is e^{-2} times the peak value. The maximum pulse energy on the sample was 34 μJ at 263 nm and 25 μJ at 211 nm with a pulse duration of about 25 ps. The pulse energy can be continuously varied by rotating the polarization of the laser beam with a half-wave plate. The uncertainty in the fluence measurement on the target was estimated within ±20%. Less than 10% of the total pulse energy was in the low intensity prepulses and post pulses at 1,053 nm. Therefore, the fraction of energy in these side pulses was negligible in the pulse train of the fourth and fifth harmonics.

Experiments were performed with two human eye bank eyes and with two freshly enucleated rabbit eyes. The human eyes were ablated within 24 hours postmortem, and the rabbit corneas were ablated within 30 hours after sacrific-

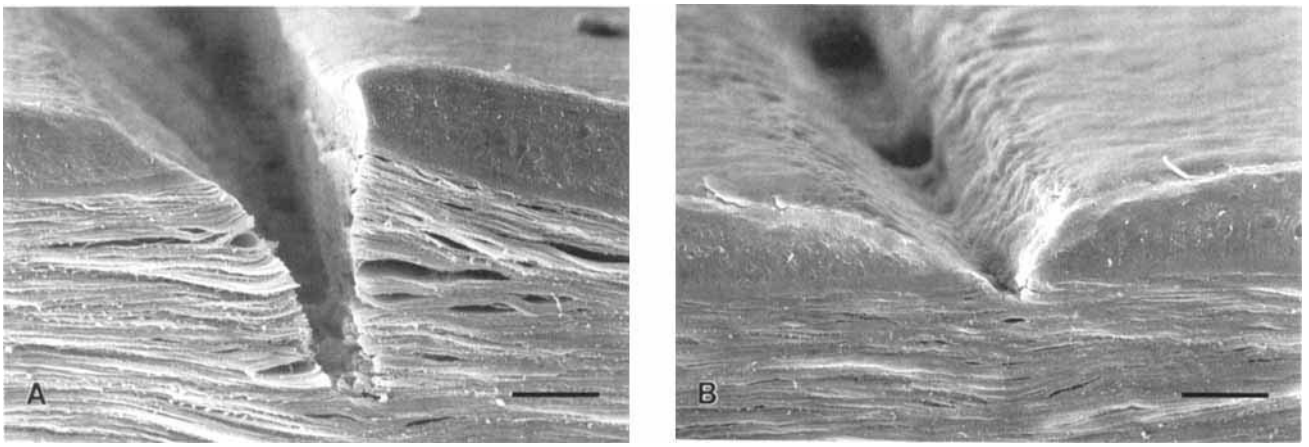

Fig. 2. SEM photographs of a human cornea ablated by 25 ps pulses. Bar = 30 μm. **A:** wavelength λ = 211 nm, spot diameter d = 60 μm, and laser fluence F = 646 mJ/cm^2. **B:** λ = 263 nm, d = 60 μm, and F = 622 mJ/cm^2.

ing the animals. The eye globe under study was held by a suction holder and the laser beam was focused onto the central area of the cornea. Since the depth of focus is much larger than the corneal thickness, the variation in the spot diameter as the beam ablates into a cornea can be neglected. The cornea was sprayed at times with a balanced salt solution to keep it moist between ablations. A linear translator, controlled by a stepping motor, was used to move the eye continuously at a constant speed in a direction perpendicular to the laser beam. The number of laser pulses per spot was determined by the speed of the translator and the size of the focal spot.

Linear incisions with a length of 1.5 mm were made on the surface of central cornea. The wavelength, pulse energy, and spot diameter were varied to investigate the dependence of the etch rate or etch depth per pulse on these parameters. To minimize the effect of varying tissue conditions, experimental results shown in each of the following figures, except in the insert in Figure 5, were obtained from the same cornea in the same experimental run. An experiment, run typically, lasted less than half an hour. After laser ablation the corneas were immediately dissected from the eye globe and fixed in a 0.6% paraformaldehyde, 1.3% glutaraldehyde, 0.06 M sodium phosphate buffer solution. These ablated corneas were later prepared for scanning electron microscopy (SEM) and TEM with standard procedures [19]. The etch depth of ablation was measured by SEM and the morphological examination of collateral tissue damage was performed by TEM.

RESULTS

Figure 2 shows representative SEM photographs of an ablated human cornea at wavelengths of 211 and 263 nm. The etch depth can be measured accurately from SEM as a percentage of the corneal thickness. The etch depth was then converted into micrometer units by assuming that the thickness of the central area equals 520 μm for human cornea and 400 μm for rabbit cornea [15]. One rabbit cornea was ablated and used to characterize the collateral tissue damage near the ablation sites in the stroma by TEM. Six linear incisions deep into stroma, with a spot diameter of 60 μm and the fluence between 300 mJ/cm^2 and 900 mJ/cm^2, were made at each of the two wavelengths. After sample processing and preparation all the incisions were serially sectioned and analyzed by TEM. Two typical photographs are displayed in Figure 3. We have determined that the size of collateral damage zone varies from 0.1 to 0.8 μm for the ablation at 211 nm and from 3 to 10 μm at 263 nm. The neatly cut collagen lamellas at the edge of the ablation site made at 211 nm were consistently observed in all TEM photographs and are in strong contrast to the severely disrupted collagen fibrils made with 263 nm. These observations agree with previous results obtained with nanosecond pulses in this spectral region [5,12] and will be discussed later. We also observed that the appearance of the collateral damage zone was not sensitive to the laser pulse energy.

The etch rate curves of human cornea as

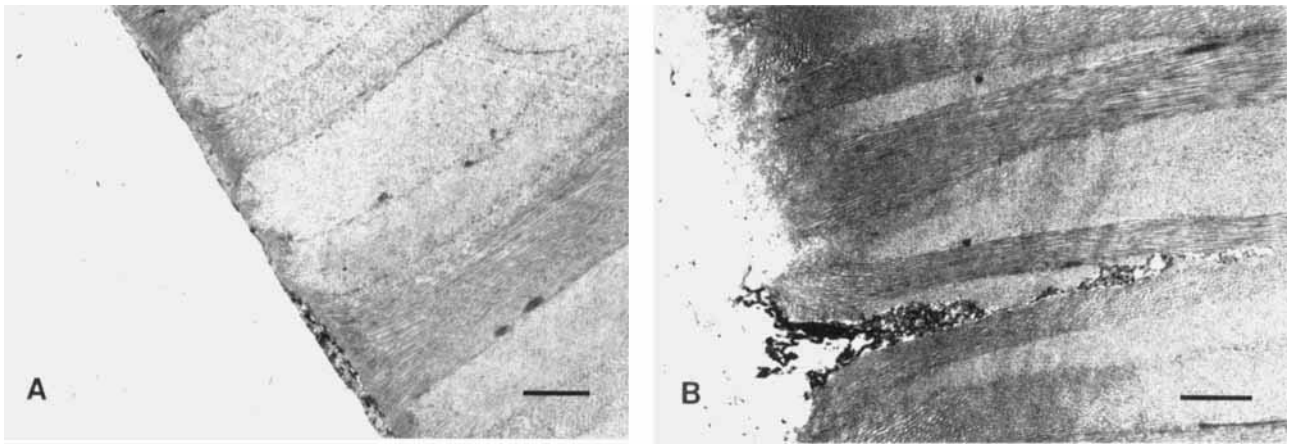

Fig. 3. TEM photographs of the stroma of a rabbit cornea ablated by 25 ps pulses. Bar = 2 μm. **A:** λ = 211 nm, d = 60 μm, and F = 540 mJ/cm^2. **B:** λ = 263 nm, d = 60 μm, and F = 860 mJ/cm^2.

functions of laser fluence at 211 nm and 263 nm are shown in Figure 4. The focal spot was measured to be 60 μm in diameter, which results in relatively large values of fluence up to about 700 mJ/cm^2 at 211 nm and 900 mJ/cm^2 at 263 nm. As shown in Figure 4, the ablation efficiency at 211 nm increase faster than that at 263 nm as the fluence rises from about 70 mJ/cm^2 and remains higher throughout the fluence range. Large focal spots of a few hundred micrometers in diameter were used to obtain the etch rate curves of human cornea with laser pulses at the 211 nm wavelength. The results are displayed in Figure 5.

To compare the effect of different spot diameter on the ablation efficiency at 211 nm we plotted the combined data of Figures 4 and 5 in the insert in Figure 5 on a log-log scale. It can be seen from the insert in Figure 5 that data groups of different spot diameters are quite consistent with each other, considering the experimental error in determining the fluence. Therefore, a single parameter, the laser fluence, may be used to describe the energy density without reference to the specific geometry, at least in the observed range of the spot diameter.

The fluence threshold of laser ablation was determined to be about 3.0 mJ/cm^2 for human cornea at 211 nm. The threshold was obtained by extrapolating the etch rate curve towards the fluence axis. The use of extrapolation was to maintain consistency between the ablation thresholds determined in different experimental runs, for example, from etch rate curves in Figures 5 and 6. The thresholds obtained by extrapolation agreed with the thresholds estimated by observation of

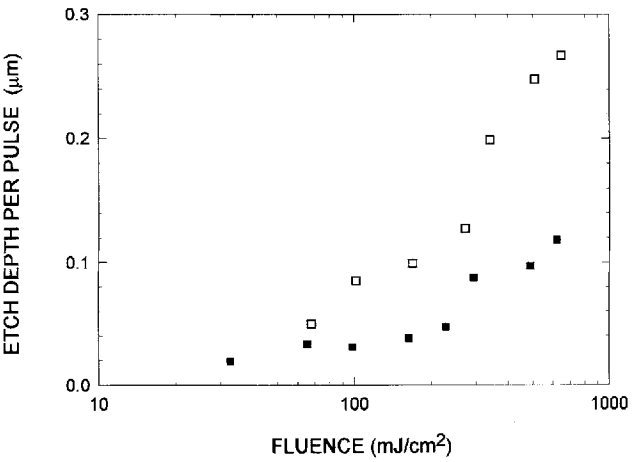

Fig. 4. Etch depth per pulse vs. laser fluence on a human cornea at different wavelengths: λ = 211 nm (hollow square) and λ = 263 nm (solid square). The spot diameter d = 60 μm with 800 pulses/spot.

minimum pulse energy required to induce sparks at the surface of a corneal sample. In addition, we would like to point out that a large number of pulses per spot were used in the present and excimer laser experiments to increase the sensitivity of the threshold measurement. Therefore, comparison of the ablation thresholds obtained in the present experiment and of those obtained by excimer lasers [4,5] is appropriate as far as the measurement method is concerned. The etch rate curves were also measured on a rabbit cornea at different wavelengths, and the results are plotted in Figure 6. The fluence thresholds for the rabbit cornea were determined to be about 2.3 mJ/cm^2 at

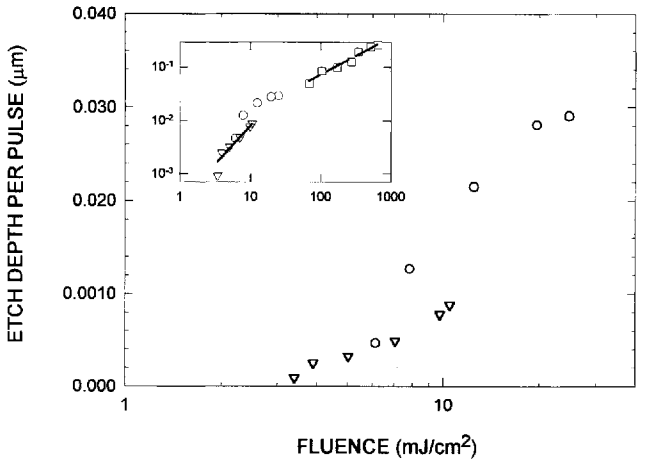

Fig. 5. Etch depth per pulse versus laser fluence on another human cornea at 211 nm with different spot diameter: 300 μm with 7200 pulses/spot (circle) and 520 μm with 12,500 pulses/spot (triangle). **Insert:** The combination of etch rate at 211 nm from Figures 4 and 5 vs. laser fluence on a log-log scale. The straight lines are the best fits to data with the same spot diameter on the log-log scale and the slope is $\bar{n}$ = 1.47 (solid line); $\bar{n}$ = 0.72 (dashed line).

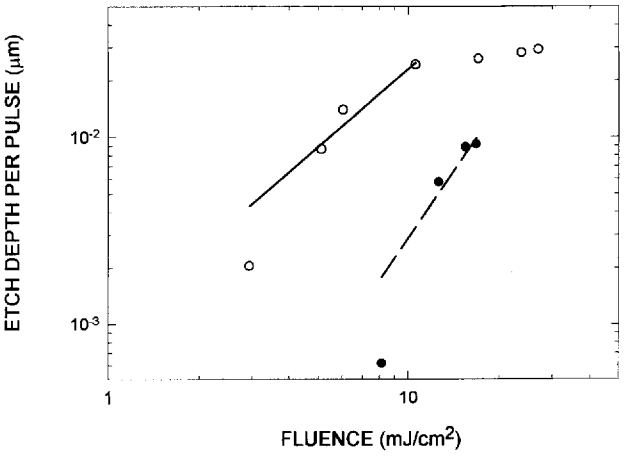

Fig. 6. Etch depth per pulse vs. laser fluence on one rabbit cornea on a log-log scale: λ = 211 nm and d = 300 μm with 7200 pulses/spot (hollow circle); λ = 263 nm and d = 600 μm with 14,400 pulses/spot (solid circle). The straight lines are the best fits to the four data points near the threshold on the log-log scale and the slope is $\bar{n}$ = 1.38 (solid line); $\bar{n}$ = 2.36 (dashed line).

211 nm and 8.0 mJ/cm^2 at 263 nm. The ablation efficiency at 211 nm is also higher than that at 263 nm in the full range of fluence investigated. This demonstrates that the picosecond UV pulses at 211 nm wavelength ablates corneal tissues more efficiently than that at 263 nm.

Despite the experimental fact that the etch rate curve is not a straight line on a log-log scale, the average slope of curve can be determined in different ranges of fluence. The slope is defined by

$$n = \frac{\Delta(\log d)}{\Delta(\log F)},$$

where d is the etch depth and F the laser fluence. In determining the average slope, $\bar{n}$, we obtained the best fit of a straight line to those data points with the same spot diameter on the log-log scale. Thus the average slope was determined by the dependence of etch rate on pulse energy and was independent of measurement accuracy of the spot diameter. For the ablation of the human cornea at 211 nm, we obtained $\bar{n}$ = 1.47 near threshold, which decreases to 0.72 when the fluence approaches the high end of the range, shown by the solid and dashed lines in the insert in Figure 5. A similar value of slope near the threshold can be found from Figure 6 for the ablation of rabbit cornea at 211 nm as $\bar{n}$ = 1.38, while $\bar{n}$ = 2.36 at 263 nm. We would like to point out that in the range near the threshold, our results are in reasonable agreement with previous results of plasma-mediated ablation on the corneal surface by the visible and near-infrared laser pulses, which ranges from $\bar{n}$ = 1.4 to $\bar{n}$ = 2 [20,21].

DISCUSSION

Since the 1 kHz repetition rate used in the present experiment was much higher than those used in the previous experiments [3–6,12], it is important to discuss the influence of the thermal relaxation of the tissue on our data. The effect of the repetition rate on the ablation threshold has been investigated with excimer lasers [4]. As the repetition rate increases from 1 Hz to 25 Hz, the ratio of the threshold at 248 nm and at 193 nm decreases from 3.7 to 1.5 due to reduction of the threshold at 248 nm. This result is qualitatively consistent with a simplified thermal model [22]. Using this model, the thermal decay times of the heated tissue are calculated to be 2 ms and 10 ms for a laser pulse at 248 nm and 193 nm, respectively. In the present experiment the ratio of threshold at 263 nm and 211 nm was measured to be 3.5. This is very close to the ratio of 3.7 measured by excimer lasers at similar wavelengths but at a 1 Hz repetition rate [4]. Additionally, the pulse energy used in the present study was at least two orders of magnitude smaller than that used in previous experiments [4,5,12]. Based on these facts, it is plausible to assume that the tis-

sue was thermally relaxed between two consecutive pulses in our experiments, at least to the extent that it was observed with excimer lasers at a 1 Hz repetition rate [4].

Figure 3 shows that the size of the collateral damage zone at the edge of ablation site increases by an order of magnitude as the wavelength of laser pulse is raised from 211 nm to 263 nm. Similar results have been obtained with nanosecond pulses as the wavelength is increased from 193 nm to 248 nm[5] or from 213 nm to 266 nm [12]. In comparison, the difference in the size and appearance of the damage zone between the ablation at 211 nm with picosecond pulses and at 193 nm or at 213 nm with nanosecond pulses was negligible. The same was observed when the damage zone created by the ablation at 263 nm was compared with that at 248 nm or 266 nm [5,12]. Two conclusions can be drawn from these observations. First the collateral tissue damage near the ablation site is not sensitive to the pulse duration in the observed range of 10^{-8} s to 10^{-11} s and to the pulse energy, as noted in the previous section. Consequently, the size of the collateral damage zone is mainly determined by the corneal absorption of optical radiation at different wavelengths. Heat conduction from the ablation site into the surrounding area may play a secondary role. Thus the collateral tissue damage may be interpreted by the photochemical model. Secondly, the corneal absorption varies in different ways in the spectral region concerned in this paper. A drastic change in the size of the damage zone occurs as the wavelength of laser pulses decreases from 248 nm to 213 nm. One must conclude from this fact that the corneal absorption increases steeply in the wavelength region from 248 nm to 213 nm. In contrast, the corneal absorption should remain about the same, which is weak in the region between 266 nm and 248 nm and strong between 213 nm and 193 nm. Accordingly, the spectral region between 193 nm and 266 nm can be divided into three smaller regions. This picture is consistent with a partial spectrum of corneal absorption measured earlier [5].

The ablation threshold changes significantly as the pulse duration decreases from about 12 ns to 25 ps. At 193 nm the fluence thresholds of ablation have been measured to be about 46 mJ/cm^2 on human cornea [5] and 50 mJ/cm^2 of calf cornea [4] with laser pulses of about 12 ns in duration. Comparing the results with human corneas [5] to ours at 211 nm, a reducton by a factor of about 15 was achieved in the ablation threshold. As discussed earlier, we can assume that the absorption of cornea at 193 nm and 211 nm was about the same. Thus the change in the threshold could only be attributed to the difference in the pulse duration. From this comparison we notice that the ratio of the fluence threshold scales with the ratio of pulse duration with an exponential factor m = 0.44, that is,

$$\frac{F_t(12\text{ ns})}{F_t(25\text{ ps})} = \left(\frac{12000}{25}\right)^{0.44},$$

where F_t is the fluence threshold. Similarly, an order of magnitude decrease in the fluence threshold is also achieved when results on calf corneas [4] are compared with our result on the rabbit cornea at both wavelengths. The factor m is about 0.50 for results at 193 nm wavelength and a 1 Hz repetition rate vs. ours at 211 nm and that at 248 nm and 1 Hz vs. ours at 263 nm [4]. One should note that the sensitivity of the fluence threshold on pulse duration in the case of corneal ablation has not been observed in the ablation of polymers by UV laser pulses. For example, it has been reported that the fluence threshold for the ablation of PMMA at 248 nm wavelength decreases only by a factor of 5 as the pulse duration changes from 16 ns to 300 fs [23].

The exponential factor m has been measured in the surface ablation of cornea, which is about 0.46 by visible laser pulses in the range of pulse duration from 8 ns to 100 fs [20] and about 0.5 by visible and near-infrared laser pulses in the range of 50 ps to 120 fs [24]. Furthermore, it has been derived that a plasma formation, induced by either cascade ionization or multiphoton ionization, could provide a scaling relation of m = 0.5 between the fluence threshold and the pulse duration in the laser-induced breakdown in transparent dielectrics [25,26]. Another similarity between the surface ablation of cornea by visible and near-infrared and UV laser pulses about the slope of etch rate curves has been identified in the last section. The corneal ablation by visible and near-infrared laser pulses with a duration of less than 10^{-7}s has been widely recognized as a result of optical breakdown with a subsequent plasma formation and has been termed a plasma-mediated ablation process [20]. In the spectral region from visible to near-infrared, the linear absorption of the laser radiation by cornea is very weak. It has been accepted that in this case the ablation is made possible only when a plasma is formed, as

the fluence increases above the threshold, which has a much stronger absorption of the laser radiation. A simple model based on the plasma absorption has been given to account for the measured slope of etch rate curve, $\bar{n}$, by assuming the nonlinear absorption of laser radiation by plasma at the wavelength of 1.05 μm [21].

Based on the similarities discussed earlier, we suggest that plasma formation may occur in corneal ablation by UV laser pulses and the threshold is determined by the appearance of plasma. When the laser fluence is below the ablation threshold the linear absorption by chromophores in the corneal matrix is the main mechanism of photon absorption [27]. As the laser fluence approaches the threshold the absorption by the water becomes more and more important because of the increased probability of nonlinear effects and other mechanisms. At the threshold the probability of the creation of high-energy free electrons is large enough that cascade ionization is initiated and a plasma is formed. The absorption of laser radiation above the threshold is due both to the plasma and chromophores, and the ablation is dominated by the action of plasma. As the fluence level rises, the absorption by plasma may increase faster than linear absorption by the chromophores. The main difference in the surface ablation of cornea by the very short laser pulses in different spectral regions may be due to the fact that the chromophore absorption of UV radiation significantly reduces the threshold for pulses of similar duration.

With this model we may interpret the exponential factors $\bar{n}$ and m discussed previously as an indication of the essential role played by plasma in corneal ablation with very short laser pulses. This model could also be used to explain the weak dependence of the factor $\bar{n}$ on the wavelength. This is due to the fact that $\bar{n}$ is related to the power with which the plasma absorption depends on the pulse energy, which has been shown to be independent of wavelength [21]. It is not clear, though, why a small value of the facter $\bar{n}$ (about 0.7) has been measured when the fluence approaches its high end. We can also use the model to qualitatively understand the LIF measurements discussed earlier. For example, the different LIF spectra measured below or above the ablation threshold [10,11] can be attributed to the appearance of the plasma. When the fluence is below the ablation threshold, the LIF results from radiative relaxation of excited molecules by chromophore absorption and have some features that are related to the energy distribution of the excited molecules. In comparison, the LIF from cornea ablated at a fluence level significantly higher than the threshold may be dominated by the quasi-blackbody radiation and radiation of ionized particles from the plasma, which has a temperature on the order of a thousand degrees. When the laser fluence is moderately higher than the threshold, the LIF consists of fluorescence from excited molecules and from plasma, and thus may be different from the LIF observed from water [16]. Finally we briefly comment on the high pressure observed in cornea at about 100 atm at a distance of 30 μm [7] and the shock wave observed in air [28] in corneal ablation by excimer lasers at 193 nm. With our model these phenomena can be interpreted as a result of acoustic waves that are generated by the cooling of plasma.

ACKNOWLEDGMENTS

The authors thank M. Costello for his work in the processing of ablated tissue samples and electron microscopy.

REFERENCES

1. Taboada J, Archibald CJ. An extreme sensitivity in the corneal epithelium to far UV ArF excimer laser pulses. Proc Aerospace Med Assoc 1981, p 8.
2. Trokel SL, Srinivasan R, Braren BB. Excimer laser surgery of the cornea. Am J Ophthalmol 1983; 96:710–714.
3. Krueger RR, Trokel SL. Quantitation of corneal ablation by ultraviolet laser light. Arch Ophthalmol 1985; 103: 1741–1742.
4. Krueger RR, Trokel SL, Schubert HD. Interaction of ultraviolet laser light with the cornea. Inves Ophthalmol Vis Sci 1985; 26:1455–1464.
5. Puliafito CA, Steinert RF, Deutsch TF, Hillenkamp F, Dehm EJ, Adler CM. Excimer laser ablation of the cornea and lens: Experimental studies. Ophthalmology 1985; 92: 741–748.
6. Puliafito CA, Wong K, Steinert RF. Quantitative and ultrastructural studies of excimer laser ablation of the cornea at 193 and 248 nanometers. Lasers Surg Med 1987; 7:155–159.
7. Srinivasan R, Dyer PE, Braren B. Far-ultraviolet laser ablation of the cornea: Photoacoustic studies. Lasers Surg Med 1987; 6:514–519.
8. Srinivasan R, Sutcliffe E. Dynamic of the ultraviolet laser ablation of corneal tissue. Am J Ophthal 1987; 103: 470–471.
9. Kitai MS, Popkov VI, Semchishen VA, Kharizov AA. The physics of UV laser cornea ablation. IEEE J Quant Electron 1991; 27:302–307.
10. Tuft S, Al-Dhahir R, Dyer P, Zhu ZH. Characterization of the fluorescence spectra produced by excimer laser irradiation of the cornea. Invest Ophthalmol Vis Sci 1990; 31:1512–1518.
11. Ediger MN. Excimer-laser-induced fluorescence of rabbit

cornea: Radiometric measurement through the cornea. Lasers Surg Med 1991; 11:93–98.
12. Ren Q, Gailitis RP, Thompson KP, Lin JT. Ablation of the cornea and synthetic polymers using a UV (213nm) solid state lasers. IEEE J Quan Electron 1990; 26:2284–2288.
13. Srinivasan R, Braren B, Dreyfus RW, Hadel L, Seeger DE. Mechanism of the ultraviolet laser ablation of polymethyl methacrylate at 193nm and 248nm: Laser-induced fluorescence analysis, chemical analysis, and doping studies. J Opt Soc Am B 1986; 3:785–791.
14. Sutcliffe E, Srinivasan R. Dynamics of UV laser ablation of polymers surfaces. J Appl Phys 1986; 60:3315–3322.
15. Maurice DM. The Cornea and Sclera. In: Davison H, ed. "The Eye," 3rd ed. New York: Academic Press, 1984:1–158.
16. Barnes PA, Rieckhoff KE. Laser induced underwater sparks. Appl Phys Lett 1968; 13:282–284.
17. Lubatschowski H, Kermani O, Otten C, Haller A, Schmiedt KC, Ertmer W. Ar-F excimer laser-induced secondary radiation in photoablation of biological tissue. Lasers Surg Med 1994; 14:168–177.
18. Chen CT, Fan YX, Eckardt RC, Byer RL. Recent developments in barium borate. Proc SPIE 1986; 681:12–19.
19. Hayat MA. "Principles and Techniques of Electron Microscopy." New York: Van Nostrand Reinhold, 1970:335–351.
20. Stern D, Schoenlein RW, Puliafito CA, Dobi ET, Birngruber R, Fujimoto JG. Corneal ablation by nanosecond, picosecond, and femtosecond lasers at 532 and 625nm Arch Ophthalmol 1989; 107:587–592.
21. Niemz MH, Klancnik EG, Bille JF. Plasma-mediated ablation of cornea tissue at 1053nm using Nd:YLF oscillator/regenerative amplifier laser. Lasers Surg Med 1991; 11:426–431.
22. van Gemert MJC, Welch AJ. Time constants in thermal laser medicine. Lasers Surg Med 1989; 9:405.
23. Kuper S, Stuke M. Femtosecond uv excimer laser ablation. Appl Phys B 1987; 44:199–204.
24. Niemz MH, Hoppeler TP, Juhasz T, Bille JF. Intrastromal ablation for refractive corneal surgery using picosecond laser pulses. Lasers Light Ophthalmol 1993; 5:149–155.
25. Fradin DW, Bloembergen N, Letellier JP. Dependence of laser-induced breakdown field strength on pulse duration. Appl Phys Lett 1973; 22:635–637.
26. Braulich P, Schmid A, Kelly P. Contributions of multiphoton absorption to laser-induced intrinsic damage in NaCl. Appl Phys Lett 1975; 26:150–153.
27. Krauss JM, Puliafito CA, Steinert RF. Laser interaction with the cornea. Surv Ophthalmol 1986; 31:37–53.
28. Bor Z, Hopp B, Racz B, Szabo G, Ratkay I, Suveges I, Fust A, Mohay J. Plume emission, shock wave and surface wave formation during excimer laser ablation of the cornea. Refractive Corneal Surg 1993; 9:S111–S115.